Author Manuscript

Author Manuscript

Author Manuscript

Author Manuscript

Advances in Imaging: Brain Tumors to Alzheimer's Disease

Rameshwar Patil, MD[1], **Yosef Koronyo, MD**[1], **Alexander V. Ljubimov, MD**[1,2], **Brenda Salumbides, MD**[1], **Adam Mamelak, MD**[1], **Pallavi R. Gangalum, MD**[1], **Hui Ding, MD**[1], **Jose Portilla-Arias, MD**[1], **Eggehard Holler, MD**[1,3], **Pramod Butte, MD**[1], **Maya Koronyo-Hamaoui, MD**[1,2], **Julia Y. Ljubimova, MD**[1,2,3], and **Keith L. Black, MD**[1,3]

[1]Department of Neurosurgery, Cedars-Sinai Medical Center, Los Angeles, California, USA.

[2]Department of Biomedical Sciences, Cedars-Sinai Medical Center, Los Angeles, California, USA.

[3]Samuel Oschin Comprehensive Cancer Center, Cedars-Sinai Medical Center, Los Angeles, California, USA.

Editor Note

Professor Black and colleagues have been working to improve the quality and sensitivity of imaging in the early detection of conditions from brain tumors to Alzheimer's disease to enhance treatment protocols and patient management. Professor Black et al introduced nanoparticles to improve MRI imaging. These nanoparticles consist of poly (b-L- malic acid (PMLA)) conjugates with monoclonal antibodies ((mAbs)) and Gd-DOTA. These are known as MRI nano-imaging agents (NIA). Most importantly, they can penetrate the endothelial blood-brain barrier (BBB) to reach brain tumors (primary or metastasis). This is effective in cases of brain tumors or breast cancer or other cancers such as lung cancer and gastric cancer having HER2 and/or EGFR positive crossing BBB. By the covalent conjugation of MR contrast (NIA), the MRI virtual biopsy can differentiate brain tumors from infections or other brain pathological conditions. The brain's intrinsic natural fluorescence such as NADH, FAD, lipopigments and porphyrin in the brain tissue can be identified by using time resolved fluorescence spectroscopy (TRFS) which is operated through the use of ultra-short laser. TRFS produces various color bands to differentiate the tumor from normal brain tissue in real time and registers the data on a 3D map. This is significant, as this will provide a greatly improved assessment methodology of tissue type. Consequently, this will potentially result in shorter operation times as well as more satisfactory tumor removal. In the detection of Alzheimer disease, amyloid plaque is deposited in retina tissue (including the RGC, RNFL and inner plexiform layer) which can produce a fluorescence effect by using curcumin as a contrast. This is then shown by human retina amyloid imaging device. Immunotherapies with glatiramer acetate (GA) have been shown to reduce amyloid deposits in brain and retinal AB deposits in mice. The study of advanced imaging technology and techniques including NIA, TRFS and the detection of amyloid plaque in Alzheimer disease are very important approaches to create a new era for diagnostic and therapeutic management of brain tumors and other cancers (HER2 and/or EGFR positive). This pioneering work by Professor Black, and colleagues, gives rise to a new hope for cancer patients for targeted therapy and for immunotherapies in Alzheimer's disease.

*Address Correspondence to author: Keith L. Black, MD, 127 S. San Vicente Boulevard, Suite A8224, Los Angeles, CA 90048, USA. keith.black@cshs.org.

Keywords

nanoconjugate; brain metastasis; MRI imaging; nano-medicine; blood-brain barrier; tumor treatment; tumor targeting; glioma; time-resolved fluorescence spectroscopy; in-vivo diagnosis; neurodegenerative disease; retina; amyloid plaques; senile plaques; eye; curcumin; optical imaging; prognosis; immunotherapy; vaccination

Technical and biological advances are improving early detection, classification, surgical, and medical management of a wide range of human disorders. In this publication, we will present advances using nano-molecular imaging to provide an imaging MRI molecular classification of brain tumors and time-resolved fluorescence spectroscopy to improve differentiation of normal from tumor infiltrated tissue during surgery in real-time. In this same communication, we will also present results demonstrating early detection of one of the hallmarks of Alzheimer's disease, amyloid plaques, using a non-invasive retinal scanning technique.

1. Brain tumors-Nano imaging

Brain tumors include primary and secondary deposits, and the primary deposit is relatively rare. The majority of brain metastasis (BM) are lung and breast which accounts for around 20–30% of cancer deaths annually.[1–6] 25–40% of BM originate from breast and lung cancer respectively.[7–8] Non-small cell lung cancer shows the highest incidence followed by small cell carcinoma.[8] In the case of breast cancer with overexpressing epidermal growth factor receptor-2 (HER2/neu) and triple-negative breast cancers (TNBC) but over expressing epidermal growth factor receptor-1 (EGFR) developing BM is a poor survival outcome.[9–12] The incidence of BM is increased even when the primary site is progressing well with treatment.[13,14]

Management of BM is complex because contrast enhancing lesions in the brain may represent several things, from a primary tumor metastasis, to an infection in an immunocompromised patient after chemotherapy, from postreatment radiation necrosis to a mimic (or actual) tumor recurrence. The therapeutic monoclonal antibodies (mAbs) e.g. tratuzumab (to HER2) for breast, ovarian and gastric cancer, cetuximub (to EGFR) for lung and breast cancer and rituximub (to CD20) for lymphoma are effective only for primary tumor treatment. However, they cannot penetrate the endothelial blood-brain barrier (BBB)[15] to reach brain tumors, and this is one of the causes of treatment failure.[13,16] These mAbs can, however, be used for drug delivery to the brain when they join with nano vehicles capable of efficiently crossing the BBB.[17–21] Nano vehicles are made up of MultiHance, a gadolinium (Gd)-based MRI contrast agent which is routinely used and is highly effective in detecting brain tumors. We have engineered a second, a new class of MR nanoimaging agents (NIA) based on poly (beta-L-malic acid)(PMLA) as a platform with a lack of toxicity and immunogenicity.[22] It can demonstrate high versatility for on-demand covalent conjugation of proteins, chemotherapeutic agents and imaging agents.[17,23,24] We engineered a NIA with various mAbs and conjugated these with Gd–DOTA (Figure 1) that can penetrate through the BBB. The composition of the nanoconjugate and hydrodynamic diameter/zeta potential is summarized in Table 1. When compared, MutiHance, Targeted NIA cetuximab

and non-targets NIA trastuzumab in case of EGFR+++, the findings reveal a higher contrast enhancement on Gd-DOTA/acetuximub (Alexa-680) and less enhancement on Gd-DOTA/trastuzumab (Alexa-680), with the highest contrast in the tumor at 60 minutes (Figure 2 and Figure 3).

In HER2 positive cases, with targeted NIA with trastzumab, the findings reveal increased contrast in the tumor within 50 minutes and this slightly declines at 180 min (Figure 4). This diagram shows that the nanoconjugates efficiently cross the BBB and there is high probability of a mechanism of nanodrug action on the tumor cell (Figure 5). Figure 6 demonstrates that free transtuzumab is inefficient for the treatment of metastatic brain tumors due to its inability to pass through the BBB, but when transtuzumab conjugates with PMLA, it can penetrate BBB and reach the tumor cells acting as a specific targeting antibody of HER2 and as an inhibitor to the activation of existing HER2 receptors.[24–28] The survival of the nanodrug treated in mice increased. Figure 7 demonstrates that the nanodrug can inhibit receptors in both wild and mutated EGFR.

2. Time resolved fluorescence spectroscopy (TRFS)

In its natural state, the brain tissue has natural fluorescence properties.[35–37] The main fluorosphores are NADH, FAD, lipopigments and porphyrins[38,39] (Figure 8). In general, tumors have lower fluorescence emissions when compared to normal tissue at the excitation light of 355nm wavelength and with a ratio of NADH. FAD as a signature for brain tumor differentiation.[40]

We introduced an instrument, the time revolved fluorescence spectroscopy. This operates where the tissue is excited using an ultrashort laser and the corresponding fluorescence intensity is captured, based on the fluorescence spectrum and the decay characteristics of various color bands from TRFS. The differentiation of the tumor tissue from normal brain tissue is possible in real time as TRFS is a single point detection tool. It works by incorporating a neuro-navigation system and registering 3D space. Neurosurgeons can continue carving the tumor boundary during an operation (Figure 9), and this information will allow the surgeon to identify areas the suction cannula is carving in, whether normal brain tissue or tumor.

This results in a significant impact on the assessment of tissue type and leads to improvements such as reducing operating time and waiting time for the frozen section. The TRFS system uses a 355nm laser pulse (400 ps, 5uJ/pulse) to excite the tissue fluorescence (Figure 10). We experimented with 9 patients of glioma. During the operation, the TRFS fiber optic probe was positioned above the areas of interest, glioma, normal cortex (NC), and normal white matter (WM). A total number of 35 points included 10 points of NC, 12 points of normal WM and 13 points for GBM. The linear discriminant analysis (LDA) classification has been implemented and integrated in a three-dimensional scatterogram. See Figure 11, which is identical to the areas of NC, WM and GBM by a 3D scatterogram of all 9 patients.

3. Retinal Imaging for Alzheimer's disease

Alzheimer's disease (AD) is the leading cause of dementia in the United States, and the fifth leading cause of death among the elderly,[63] claiming more than 5 million Americans.[63] It is estimated that the number of Americans affected by AD could triple by 2050.[63] The cost of medical care for AD in the US is more than $200 billion a year currently and this would increase to up to $1.1 trillion in 2050.[63] It is estimated that 44 million people are suffering from Alzheimer's disease or other dementias globally[41] and this number could increase to 76 million in 2030 and 135 million in 2050.[42,43]

Early diagnosis of AD could potentially result in early treatment or timely prevention of disease progression.

Today, a confirmation of definitive AD is only possible with an autopsy of brain tissue, with an examination for the presence of two pathological hallmark signs of AD: amyloid (senile) plaques predominantly composed of proteinaceous Aβ and neurofibrillary tangles (NFT) formed by an aggregation of the hyperphosphorylated microtubule-associated protein tau.[44,45] Cognitive tests such as the Mini Mental State Examination (MMSE) can determine level of impairment, but not the type of disease. Clinical, genetic, physiologic, and biochemical evidences suggest that the primary pathological event leading to AD is an age-dependent accumulation of toxic alloforms of Aβ in the brain.[46,47] This elevation in Aβ levels results in a self-association, formation of neurotoxic Aβ assemblies, and deposition of fibrillary Aβ in amyloid plaques. Elevated cerebral levels of Aβ seem to be a very early and specific event in AD that likely occurs 10–20 years prior to symptom manifestation.[47–50] Although methods are currently being developed to detect amyloid-related changes directly within the skull-shielded brain (i.e. PET, MRI), there are many difficulties and limitations inherent in these techniques such as low specificity, poor spatial resolution and high costs.[51–58] Presence of Aβ plaques in the retina of people with AD, possibly at pre-symptomatic stages, and the ability to detect them with high detail and accuracy offers a new improved opportunity for the early detection of AD. The retina is a part of the central nervous system, originating as an outgrowth of the developing brain and shares many similarities with the brain. The retina is easily accessible for direct and noninvasive imaging with high spatial resolution and sensitivity.[58]

In retinal imaging for AD patients, our research group at Cedars-Sinai, also founding members of Neurovision Imaging, made a groundbreaking discovery-the first identification of Aβ plaque pathology in retinas of AD patients: with definite, probable and possible diagnosis, comparable with that observed in their brains.[60] Our studies with AD transgenic mice have further shown that Aβ plaques may appear in the retina before they appear in the brain. Our group has developed an approach to detect those plaques in live rodent models with unprecedented high detail.[59,60] Retinal plaques in mice were mainly detected in the nerve fiber layer (NFL) throughout the outer plexiform layer, and their prevalence correlated with disease progression, retinal ganglion cell (RGC) degeneration, microglial activation, and functional impairment.[61] Therefore it is essential to develop a method to detect Aβ plaques in live patients by a noninvasive and direct retinal imaging with high resolution and

less expense compared to brain imaging techniques, which will enable a detailed evaluation of AD-specific pathology at an early stage.

The retina may offer a better target to detect AD pathology since existing brain-imaging technologies are radioactive, invasive and cannot provide sufficient detail about early changes in amyloid build up. A direct retinal-imaging test may offer details related to early AD pathology in real-time, including smaller-size plaque accumulation, individual plaque dynamic (appearance and clearance), plaque distribution and geographical location near retinal structures (i.e. blood vessels) that neither brain imaging nor the highly invasive CSF Ab levels currently provide. In collaboration with Carol A. Miller, MD (Pathology and Neurology, USC), we continue to collect rare retinal and brain samples isolated from AD patients at different stages of the disease. This is a unique collection of well-characterized AD patients that have both pre-mortem cognitive/behavioral and postmortem complete brain pathological assessments.

Results and Discussion

Our Cedars-Sinai research group is a pioneer in identifying the feature Aβ plaque pathology in postmortem retinas of AD patients (Figure 12), and in early-stage cases (Figure 13), comparable with plaque load observed in their brains. Retinal Aβ plaques in AD patients were found to be located mostly within the inner layers. Retinal plaques location and morphology were qualitatively documented and compared with those found in the brain. In AD patients, retinal Aβ plaques were mostly found abluminal and near blood vessels, and had typical morphology of presumably earlier-stage; condensed hard-core(s) containing aggregated Aβ and lack of radiating fibril arms, less frequently seen in the brains. These findings suggest that Aβ plaques may appear sooner in the retina than in the brain. A quantitative analysis (Figure 14) of curcumin-labeled retinal Aβ plaques in AD-Tg mice indicated a significant decrease in their number and size following immunotherapy and to the same extent as their brain counterparts. [59–60] These findings provided further evidence for a correlation between retinal and brain plaques. Moreover, curcumin was found to cross the blood-retinal and brain barriers and label Aβ with high affinity and specificity in vivo in mouse model retinas and brains. More importantly, in early stage of the disease, Aβ plaques appeared in the retina before their appearance in the brain (Figure 15). A novel noninvasive retinal imaging approach developed by our group, enabled the detection of Aβ plaques with high sensitivity, specificity, and repeatability in live AD transgenic (AD-Tg) mouse models, after intravenous (iv.) injection of curcumin or when given orally (Figure 16). A follow up study from our group demonstrated the feasibility to noninvasively monitor individual Aβ-plaque appearance and clearance in the retina of transgenic AD models in response to an immunotherapy (Figure 17). Phase I and II clinical trials using curcumin showed low toxicity profiles in humans even at high doses (8–12 gr/day), and when given over extended periods of time.[62]

Conclusion

We demonstrate several examples of imaging technologies which aim to improve detection and classification, as well as surgical and medical management of brain tumors and Alzheimer's disease.

1. Brain tumors-Nano imaging

A significant advantage of our nanosystem is that it is possibile to use not only for imaging but also for the delivery of specific mRNA suppressors (AONs) or other drugs with simple structural manipulations of nanoplatforms for efficient tumor treatment.[31,32] This versatility was illustrated here by successfully treating BMs from breast and lung tumors using different tumor-targeting mAbs (e.g., trastuzumab for HER2+ tumors and anti-human TfR for EGFR+ tumors (Figure 6). For BM treatment, Gd-DOTA in NIAs was just substituted by HER2- or EGFR-specific AONs to block the synthesis of these tumor markers along with endosomal escape units for cytoplasmic delivery and PEG for protection. These AONs were delivered to the tumor cell cytoplasm while sparing healthy brain tissue (Figure 18). They efficiently blocked the synthesis of new HER2 or EGFR, and suppressed the activation of a downstream PI3K/Akt signaling pathway. This pro-survival pathway may contribute to apoptosis prevention, regulation of cell cycle progression, and enhanced tumor cell survival.[29,30, 33–34]

2. Time resolved fluorescence spectroscopy (TRFS)

TRFS has the potential to be an extremely helpful surgical tool that will allow surgeons to more precisely identify tumor margins for a wide variety of tumors, thus, improving surgical outcomes.

3. Retinal Imaging for Alzheimer's disease

The retina is part of the central nervous system. Both the optic nerve and the retina have been shown to succumb to neurodegeneration in AD. Aβ accumulation in the retina has been well documented in AD mouse models.[60,64–66] We have successfully documented Aβ-deposits in the retina of patients with AD and MCI and APP/PS1 Tg mouse models NDD76. The original discovery of amyloid-beta plaques in the retina of AD patients at early stages[60] was followed by the demonstration of increased Abeta1–42 peptides in AD patients' retina[67] and further detection of plaque-like structures in the postmortem retina of an AD patient.[68]

The retina is easily accessible for direct and noninvasive imaging with high spatial resolution and sensitivity. Our group was the first to report that pathology in definite, probable, and possible AD patient retinas correlate with brain amyloidosis.[60] We also reported that Aβ deposits appear very early in the retina and along the blood vessels of AD transgenic mice-seemingly even before plaques appeared in the brain.[60] Several groups have shown therapeutic amyloid changes in the retinas of AD and glaucoma rodent models.[60,69,70]

Since the retina can contain autoflourescence spots, the use of amyloid binding contrast such as curcumin is critical to reliable identification of amyloid deposits in the retinal tissue. The

extensive studies performed by the Koronyo-Hamaoui team to identify and image Aβ plaque thru the retina provided the grounds to develop the human retinal amyloid imaging device.

Biographies

Rameshwar P, MD

Black KL, MD

References

1. Steeg PS, Camphausen KA, Smith QR. Brain Metastases as Preventive and Therapeutic Targets. Nat Rev Cancer. 2011; 11:352–63. [PubMed: 21472002]

2. Khanfir A, Lahiani F, Bouzguenda R, et al. Prognostic Factors and Survival in Metastatic Breast Cancer: A Single Institution Experience. Rep Pract Oncol Radiother. 2013; 18:127–32. [PubMed: 24416543]

3. Ranjan T, Abrey LE. Current Management of Metastatic Brain Disease. Neurotherapeutics. 2009; 6:598–603. [PubMed: 19560748]

4. Lu J, Steeg PS, Price JE, et al. Breast Cancer Metastasis: Challenges and Opportunities. Cancer Res. 2009; 69:4951–3. [PubMed: 19470768]

5. Vona-Davis L, Rose DP, Gadiyaram V, et al. Breast Cancer Pathology, Receptor Status, and Patterns of Metastasis in a Rural Appalachian Population. J Cancer Epidemiol. 2014; 2014:170634. [PubMed: 24527034]

6. Lin NU, Amiri-Kordestani L, Palmieri D, et al. CNS Metastases in Breast Cancer: Old Challenge, New Frontiers. Clin Cancer Res. 2013; 19:6404–18. [PubMed: 24298071]

7. Eldredge HB, Denittis A, Duhadaway JB, et al. Concurrent Whole Brain Radiotherapy and Short-Course Chloroquine in Patients with Brain Metastases: a Pilot Trial. J Radiat Oncol. 2013; 2:315–21.

8. Nayak L, Lee EQ, Wen PY. Epidemiology of Brain Metastases. Curr Oncol Rep. 2012; 14:48–54. [PubMed: 22012633]

9. Baselga J. Targeting Tyrosine Kinases in Cancer: the Second Wave. Science. 2006; 312:1175–8. [PubMed: 16728632]

10. Renfrow JJ, Lesser GJ. Molecular Subtyping of Brain Metastases and Implications for Therapy. Curr Treat Options Oncol. 2013; 14:514–27. [PubMed: 23907440]

11. Lin NU, Claus E, Sohl J, et al. Sites of Distant Recurrence and Clinical Outcomes in Patients with Metastatic Triple-Negative Breast Cancer: High Incidence of Central Nervous System Metastases. Cancer. 2008; 113:2638–45. [PubMed: 18833576]

12. Schouten LJ, Rutten J, Huveneers HA, et al. Incidence of Brain Metastases in a Cohort of Patients with Carcinoma of the Breast, Colon, Kidney, and Lung and Melanoma. Cancer. 2002; 94:2698–705. [PubMed: 12173339]

13. Brabletz T, Lyden D, Steeg PS, et al. Roadblocks to Translational Advances on Metastasis Research. Nat Med. 2013; 19:1104–9. [PubMed: 24013756]

14. Gallego Perez-Larraya J, Hildebrand J. Brain Metastases. Handb Clin Neurol. 2014; 121:1143–57. [PubMed: 24365409]

15. Jia W, Lu R, Martin TA, et al. The Role of Claudin-5 in Blood-Brain Barrier (BBB) and Brain Metastases (Review). Mol Med Repts. 2014; 9:779–85. [PubMed: 24366267]

16. Lin NU. Targeted Therapies in Brain Metastases. Curr Treat Options Neurol. 2014; 16:276. [PubMed: 24353011]

17. Inoue S, Patil R, Portilla-Arias J, et al. Nanobiopolymer for Direct Targeting and Inhibition of EGFR Expression in Triple Negative Breast Cancer. PLoS One. 2012; 7:e31070. [PubMed: 22355336]

18. Markman JL, Rekechenetskiy A, Holler E, et al. Nanomedicine Therapeutic Approaches to Overcome Cancer Drug Resistance. Adv Drug Deliv Rev. 2013; 65:1866–79. [PubMed: 24120656]

19. Pardridge WM. Blood-Brain Barrier Drug Delivery of IgG Fusion Proteins with a Transferrin Receptor Monoclonal Antibody. Expert Opin Drug Deliv. 2015; 12:207–22. [PubMed: 25138991]

20. Bickel U, Yoshikawa T, Pardridge WM. Delivery of Peptides and Proteins Through the Blood-Brain Barrier. Adv Drug Deliv Rev. 2001; 46:247–79. [PubMed: 11259843]

21. Daniels TR, Bernabeu E, Rodriguez JA, et al. The Transferrin Receptor and the Targeted Delivery of Therapeutic Agents Against Cancer. Biochim Biophys Acta. 2012; 1820:291–317. [PubMed: 21851850]

22. Ljubimova JY, Portilla-Arias J, Patil R, et al. Toxicity and Efficacy Evaluation of Multiple Targeted Polymalic Acid Conjugates for Triple-Negative Breast Cancer Treatment. J Drug Target. 2013; 21:956–67. [PubMed: 24032759]

23. Lee BS, Fujita M, Khazenzon NM, et al. Polycefin, a New Prototype of a Multifunctional Nanoconjugate Based on Poly (↕-L-Malic Acid) for Drug Delivery. Bioconjug Chem. 2006; 17:317–26. [PubMed: 16536461]

24. Inoue S, Ding H, Portilla-Arias J, et al. Polymalic Acid-Based Nanobiopolymer Provides Efficient Systemic Breast Cancer Treatment by Inhibiting Both HER2/Neu Receptor Synthesis and Activity. Cancer Res. 2011; 71:1454–64. [PubMed: 21303974]

25. Pestalozzi BC, Brignoli S. Trastuzumab in CSF. J Clin Oncol. 2000; 18:2349–51.

26. Sun M, Behrens C, Feng L, et al. HER Family Receptor Abnormalities in Lung Cancer Brain Metastases and Corresponding Primary Tumors. Clin Cancer Res. 2009; 15:4829–37. [PubMed: 19622585]

27. Hu J, Ljubimova JY, Inoue S, et al. Phosphodiesterase Type 5 Inhibitors Increase Herceptin Transport and Treatment Efficacy in Mouse Metastatic Brain Tumor Models. PLoS One. 2010; 5:e10108. [PubMed: 20419092]

28. Emlet DR, Gupta P, Holgado-Madruga M, et al. Targeting a Glioblastoma Cancer Stem-Cell Population Defined by EGF Receptor Variant III. Cancer Res. 2014; 74:1238–49. [PubMed: 24366881]

29. Moelling K, Schad K, Bosse M, et al. Regulation of Raf-Akt Cross-Talk. J Biol Chem. 2002; 277:31099–106. [PubMed: 12048182]

30. Chautard E, Ouedraogo ZG, Biau J, et al. Role of Akt in Human Malignant Glioma: from Oncogenesis to Tumor Aggressiveness. J Neurooncol. 2014; 117:205–15. [PubMed: 24477623]

31. Ding H, Inoue S, Ljubimov AV, et al. Inhibition of Brain Tumor Growth by Intravenous Poly (↕-L-Malic Acid) Nanobioconjugate with Ph-Dependent Drug Release. Proc Natl Acad Sci USA. 2010; 107:18143–8. [PubMed: 20921419]

32. Langer R, Weissleder R. Nanotechnology. JAMA. 2015; 313:135–6. [PubMed: 25585320]

33. Hatake K, Tokudome N, Ito Y. Next Generation Molecular Targeted Agents for Breast Cancer: Focus on EGFR and VEGFR Pathways. Breast Cancer. 2007; 14:132–49. [PubMed: 17485898]

34. Peddi PF, Hurvitz SA. PI3K Pathway Inhibitors for the Treatment of Brain Metastases with a Focus on HER2+ Breast Cancer. J Neurooncol. 2014; 117:7–13. [PubMed: 24469856]

35. Butte PV, Fang Q, Jo JA, et al. Intra-operative delineation of primary brain tumors using time-resolved fluorescence spectroscopy. μJ Biomed Opt§. 2010; 15:027008. [PubMed: 20459282]

36. Butte PV, Pikul BK, Hever A, et al. Diagnosis of meningioma by time-resolved fluorescence spectroscopy. J Biomed Opt. 2005; 10:064026. [PubMed: 16409091]

37. Butte PV, Mamelak AN, Nuno M, et al. Fluorescence lifetime spectroscopy for guided therapy of brain tumors. Neuroimage. 2011; 54(Suppl 1):S125–35. [PubMed: 21055475]

38. Lin WC, Toms SA, Johnson M, et al. In Vivo Brain Tumor Demarcation Using Optical Spectroscopy. μPhotochem Photobiol§. 2001; 73:396–402. [PubMed: 11332035]

39. Lin WC, Sandberg DI, Bhatia S, et al. Optical spectroscopy for in-vitro differentiation of pediatric neoplastic and epileptogenic brain lesions. μJ Biomed Opt§. 2009; 14:014028. [PubMed: 19256716]

40. Liu Q, Grant G, Li J, et al. Compact point-detection fluorescence spectroscopy system for quantifying intrinsic fluorescence redox ratio in brain cancer diagnostics. J Biomed Opt. 2011; 16:037004. [PubMed: 21456877]

41. Alzheimer's Disease International (ADI). [Accessed July 20, 2015] Policy Brief for Heads of Government The Global Impact of Dementia 2013–2050. p. 3at http://www.alz.co.uk/research/GlobalImpactDementia2013.pdf

42. Alzheimer's Disease International (ADI). [Accessed July 20, 2015] World Alzheimer Report 2010: The Global Economic Impact of Dementia. at http://www.alz.co.uk/research/world-report-2010

43. World Health Organization. [Accessed July 20, 2015] Dementia: A Public Health Priority. at http://www.who.int/mental_health/publications/dementia_report_2012

44. Hardy J, Selkoe DJ. The amyloid hypothesis of Alzheimer's disease: Progress and problems on the road to therapeutics. Science. 2002; 297:353–6. [PubMed: 12130773]

45. Trojanowski JQ, Schmidt ML, Shin RW, et al. Altered tau and neurofilament proteins in neuro-degenerative diseases: Diagnostic implications for Alzheimer's disease and lewy body dementias. Brain Pathol. 1993; 3:45–5. [PubMed: 8269083]

46. Lee VM. Regulation of tau phosphorylation in Alzheimer's disease. Ann N Y Acad Sci. 1996; 777:107–13. [PubMed: 8624072]

47. Jack CR Jr, Albert MS, Knopman DS, et al. Introduction to the recommendations from the national institute on aging-alzheimer's association workgroups on diagnostic guidelines for Alzheimer's disease. Alzheimers Dement. 2011; 7:257–62. [PubMed: 21514247]

48. Sperling RA, Aisen PS, Beckett LA, et al. Toward defining the preclinical stages of Alzheimer's disease: Recommendations from the national institute on aging-alzheimer's association workgroups on diagnostic guidelines for Alzheimer's disease. Alzheimers Dement. 2011; 7:280–92. [PubMed: 21514248]

49. Reaume AG, Howland DS, Trusko SP, et al. Enhanced amyloidogenic processing of the beta-amyloid precursor protein in gene-targeted mice bearing the swedish familial Alzheimer's disease mutations and a "Humanized" Abeta sequence. J Biol Chem. 1996; 271:23380–8. [PubMed: 8798542]

50. Holmes C, Boche D, Wilkinson D, et al. Long-term effects of abeta42 immunisation in Alzheimer's disease: Follow-up of a randomised, placebo-controlled phase i trial. Lancet. 2008; 372:216–223. [PubMed: 18640458]

51. Nordberg A. Amyloid imaging in early detection of Alzheimer's disease. Neurodegener Dis. 2010; 7:136–8. [PubMed: 20197692]

52. Klunk WE, Lopresti BJ, Ikonomovic MD, et al. Binding of the positron emission tomography tracer pittsburgh compound-b reflects the amount of amyloid-beta in Alzheimer's disease brain but not in transgenic mouse brain. J Neurosci. 2005; 25:10598–606. [PubMed: 16291932]

53. Klunk WE, Engler H, Nordberg A, et al. Imaging brain amyloid in Alzheimer's disease with pittsburgh compound-b. Ann Neurol. 2004; 55:306–19. [PubMed: 14991808]

54. Nakada T, Matsuzawa H, Igarashi H, et al. In vivo visualization of senile-plaque-like pathology in Alzheimer's disease patients by mr microscopy on a 7t system. J Neuroimaging. 2008; 18:125–9. [PubMed: 18298677]

55. Wang Y, Klunk WE, Debnath ML, et al. Development of a pet/spect agent for amyloid imaging in Alzheimer's disease. J Mol Neurosci. 2004; 24:55–62. [PubMed: 15314250]

56. Lockhart A, Lamb JR, Osredkar T, et al. Pib is a non-specific imaging marker of amyloid-beta (abeta) peptide-related cerebral amyloidosis. Brain. 2007; 130:2607–15. [PubMed: 17698496]

57. Ng S, Villemagne VL, Berlangieri S, et al. Visual assessment versus quantitative assessment of 11c-pib pet and 18f-fdg pet for detection of Alzheimer's disease. J Nucl Med. 2007; 48:547–52. [PubMed: 17401090]

58. Hintersteiner M, Enz A, Frey P, et al. In vivo detection of amyloid-beta deposits by near-infrared imaging using an oxazine-derivative probe. Nat Biotechnol. 2005; 23:577–83. [PubMed: 15834405]

59. Koronyo Y, Salumbides BC, Black KL, et al. Alzheimer's disease in the retina: imaging retinal aβ plaques for early diagnosis and therapy assessment. Neurodegener Dis. 2012; 10:285–93. [PubMed: 22343730]

60. Koronyo-Hamaoui M, Koronyo Y, Ljubimov AV, et al. Identification of amyloid plaques in retinas from Alzheimer's patients and noninvasive in vivo optical imaging of retinal plaques in a mouse model. Neuroimage. 2011; 54(Suppl 1):S204–17. [PubMed: 20550967]

61. Chiu K, Chan TF, Wu A, et al. Neurodegeneration of the retina in mouse models of Alzheimer's disease: What can we learn from the retina? μAge (Dordr)§. 2012; 34:633–49. [PubMed: 21559868]

62. Dhillon N, Aggarwal BB, Newman RA, et al. Phase ii trial of curcumin in patients with advanced pancreatic cancer. Clin Cancer Res. 2008; 14:4491–9. [PubMed: 18628464]

63. Alzheimer's and Dementia. 2015 Alzheimer's disease facts and figures. Washington, DC: Alzheimer's Association Public Policy Office; at https://www.alz.org/facts/downloads/facts_figures_2015.pdf [Accessed July 20, 2015]

64. Ning A, Cui J, To E, et al. Amyloid-beta deposits lead to retinal degeneration in a mouse model of Alzheimer disease. Invest Ophthalmol Vis Sci. 2008; 49:5136–43. [PubMed: 18566467]

65. Perez SE, Lumayag S, Kovacs B, et al. Beta-amyloid deposition and functional impairment in the retina of the APP swe/ps1DeltaE9 transgenic mouse model of Alzheimer's disease. Invest Ophthalmol Vis Sci. 2009; 50:793–800. [PubMed: 18791173]

66. Liu B, Rasool S, Yang Z, et al. Amyloid-peptide vaccinations reduce beta-amyloid plaques but exacerbate vascular deposition and inflammation in the retina of Alzheimer's transgenic mice. Am J Pathol. 2009; 175:2099–110. [PubMed: 19834067]
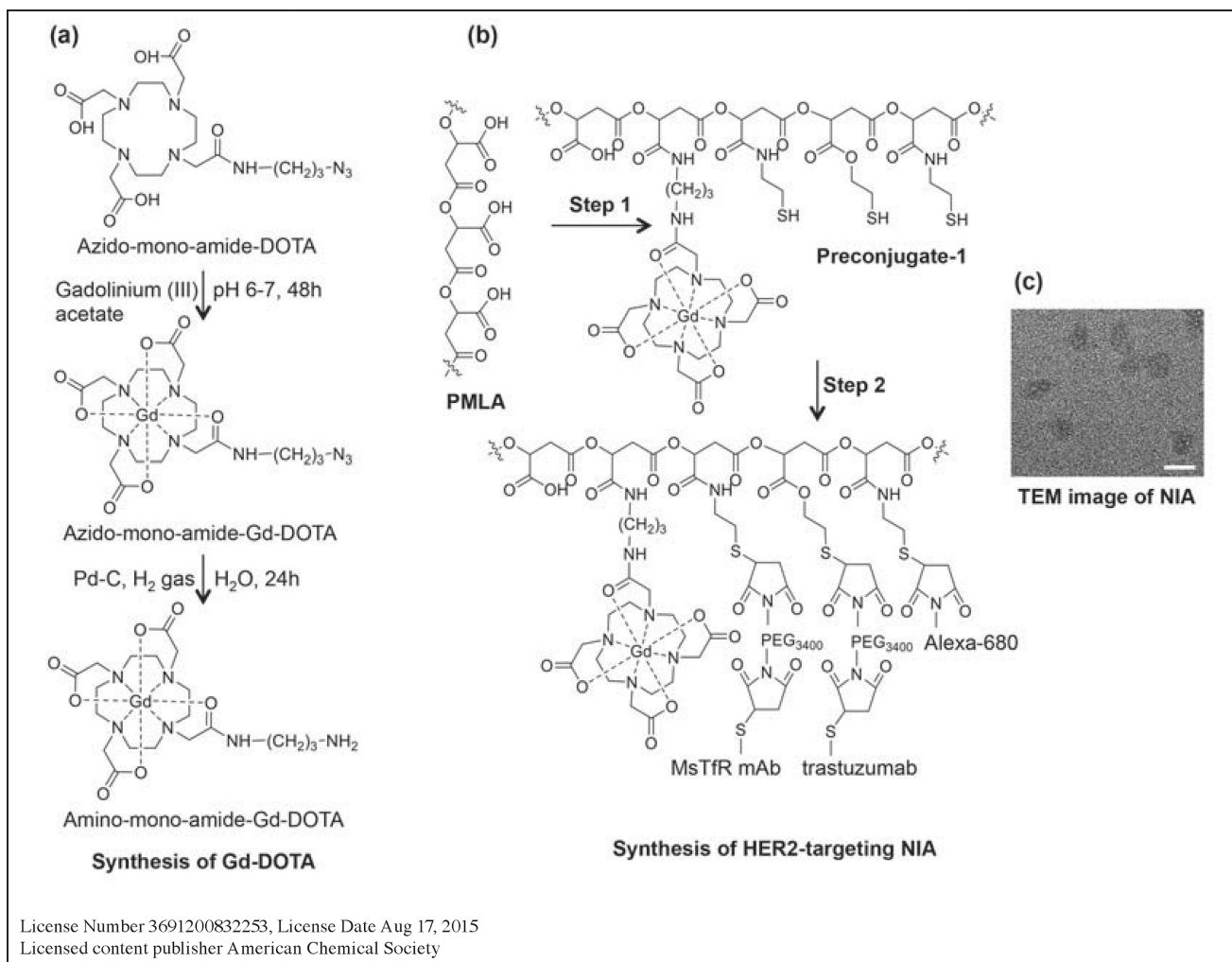
67. Alexandrov PN, Pogue A, Bhattacharjee S, et al. Retinal amyloid peptides and complement factor H in transgenic models of Alzheimer's disease. Neuroreport. 2011; 22:623–7. [PubMed: 21734608]

68. Tsai YC, Lu B, Ljubimov AV, et al. Ocular Changes in TgF344-AD Rat Model of Alzheimer's Disease. Invest Ophthalmol Vis Sci. 2014; 55:523–34. [PubMed: 24398104]

69. Guo L, Salt TE, Luong V, et al. Targeting amyloid-beta in glaucoma treatment. Proc Natl Acad Sci USA. 2007; 104:13444–9. [PubMed: 17684098]

70. Liu B, Rasool S, Yang Z, et al. Amyloid-peptide vaccinations reduce beta-amyloid plaques but exacerbate vascular deposition and inflammation in the retina of Alzheimer's transgenic mice. Am J Pathol. 2009; 175:2099–110. [PubMed: 19834067]

Figure 1.
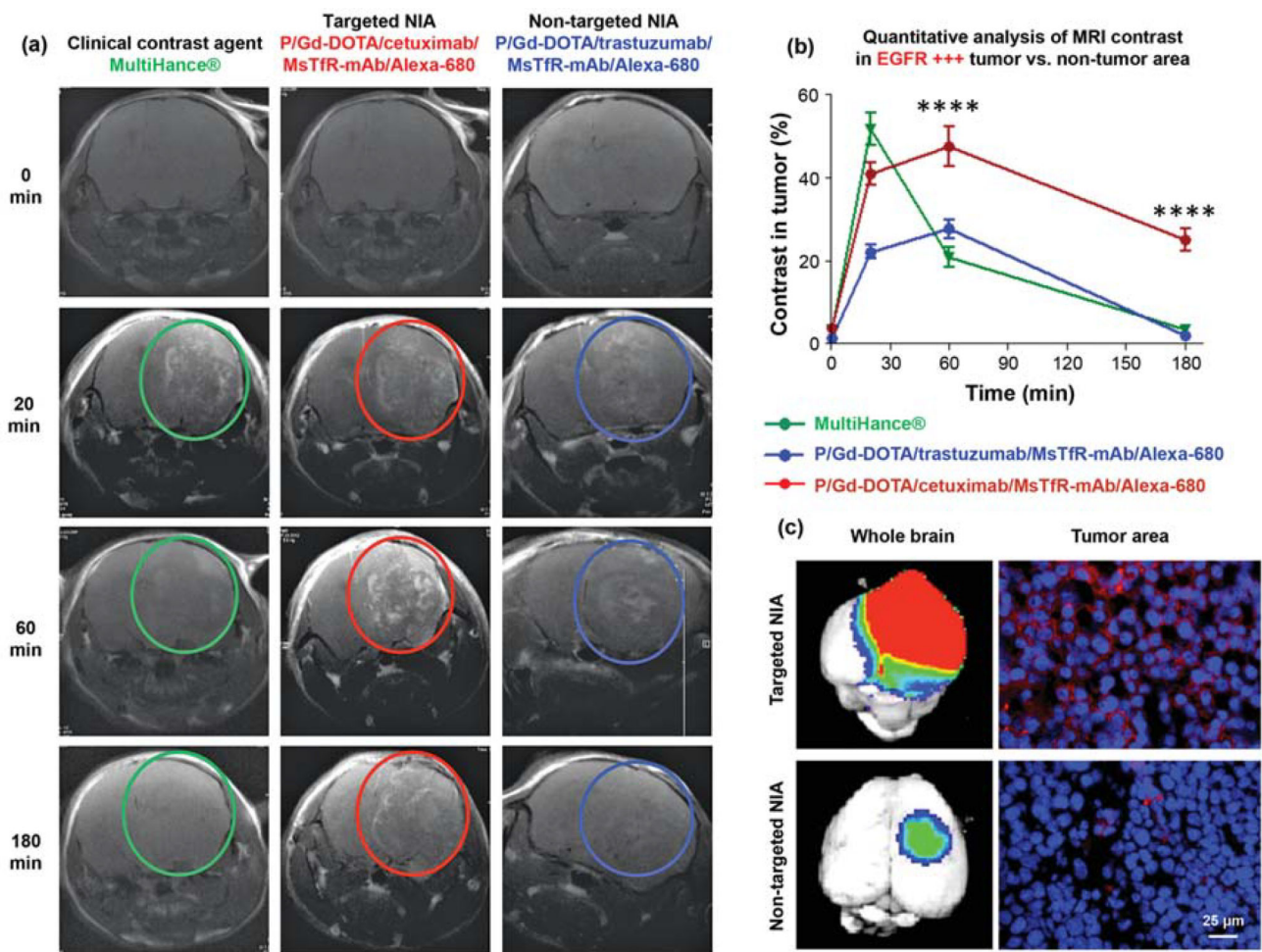
Figure 2.

License Number 3691200832253, License Date Aug 17, 2015
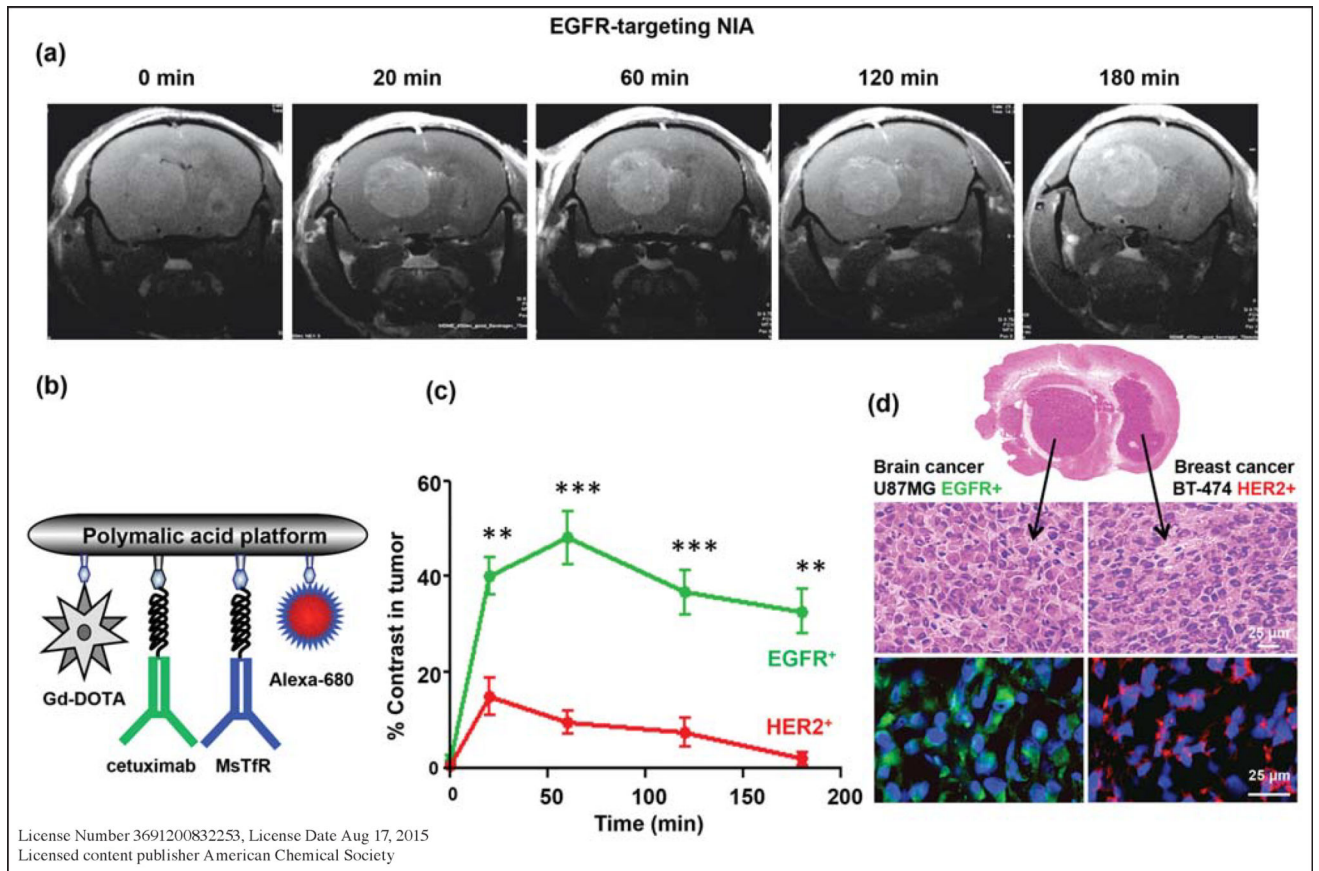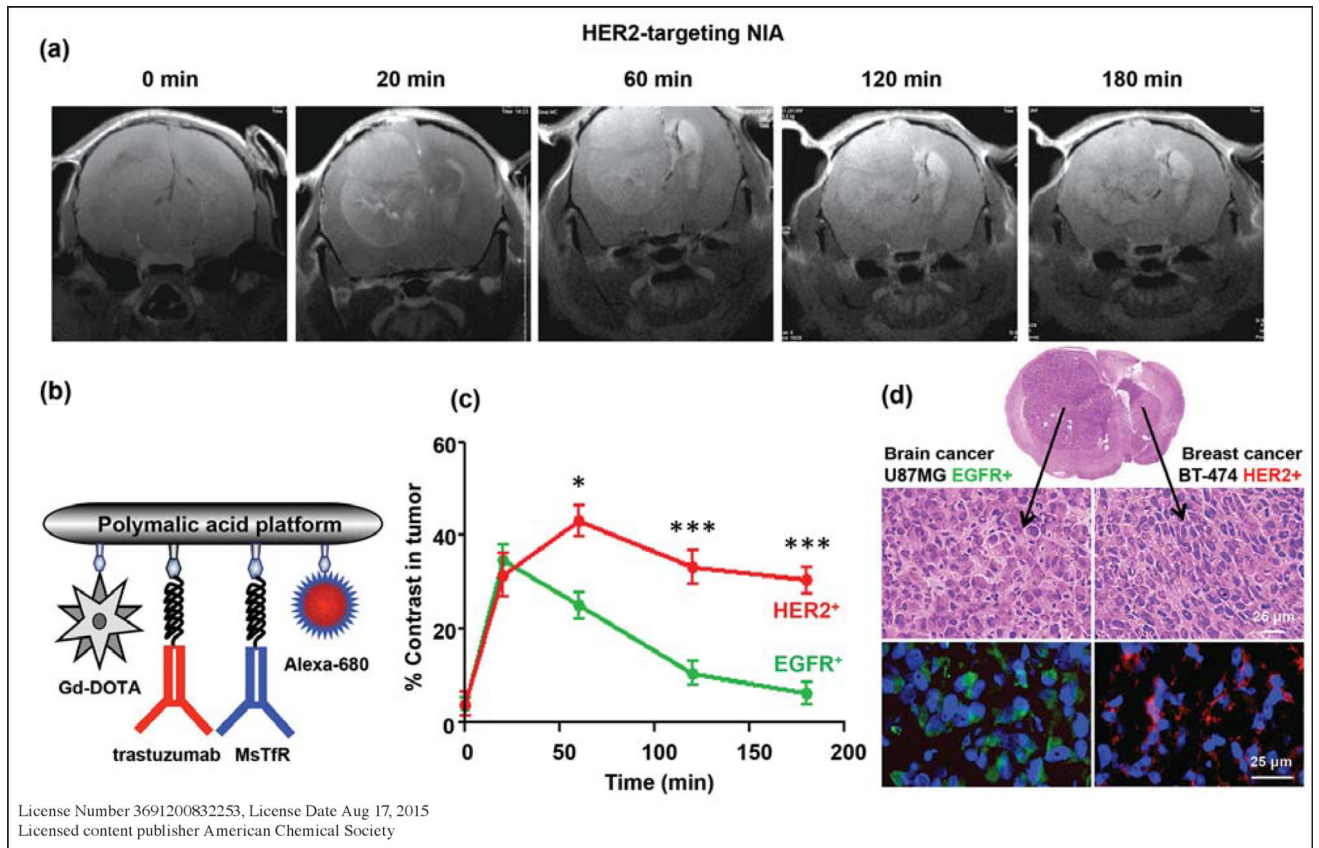Licensed content publisher American Chemical Society

Figure 3.

License Number 3691200832253, License Date Aug 17, 2015
Licensed content publisher American Chemical Society

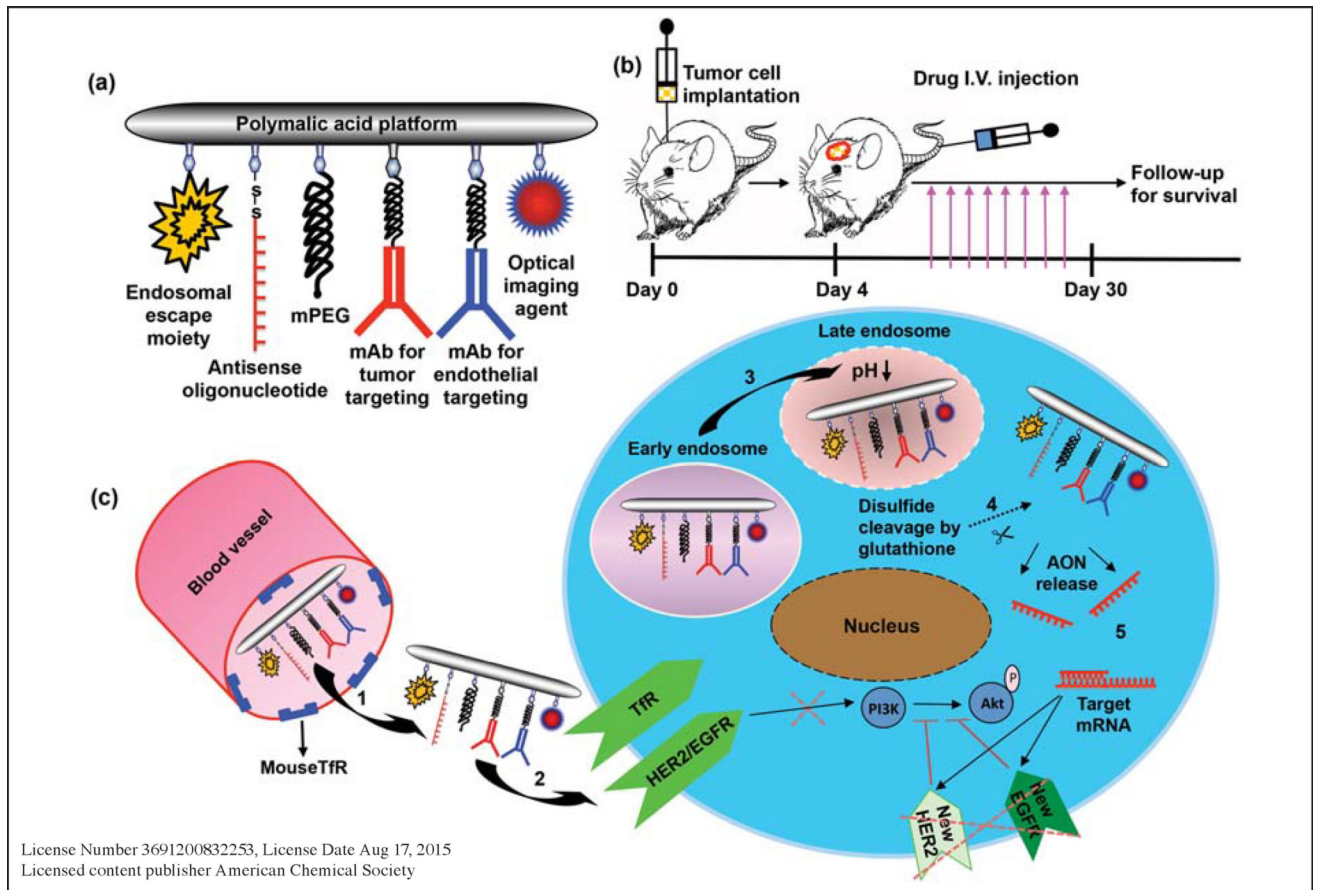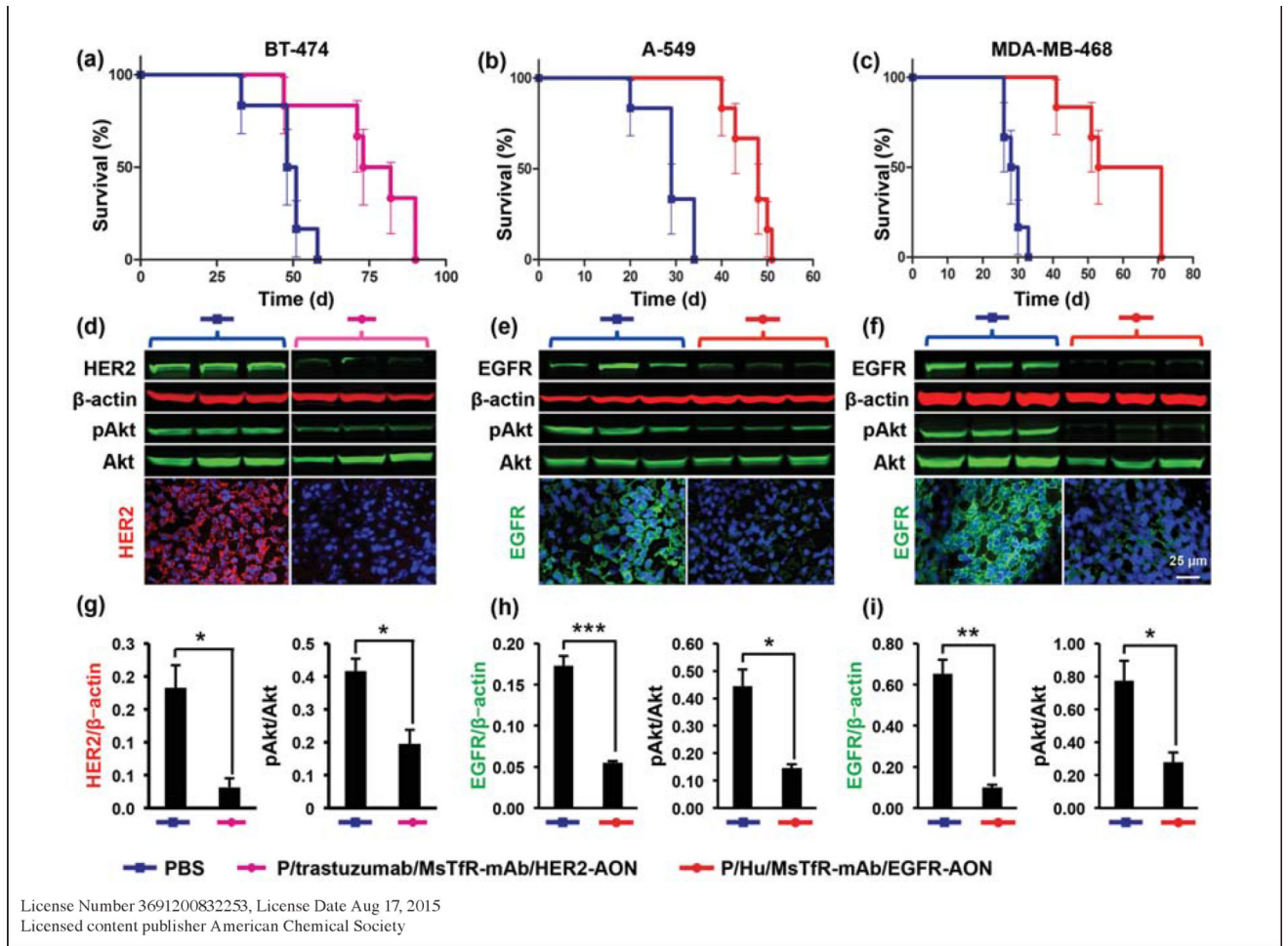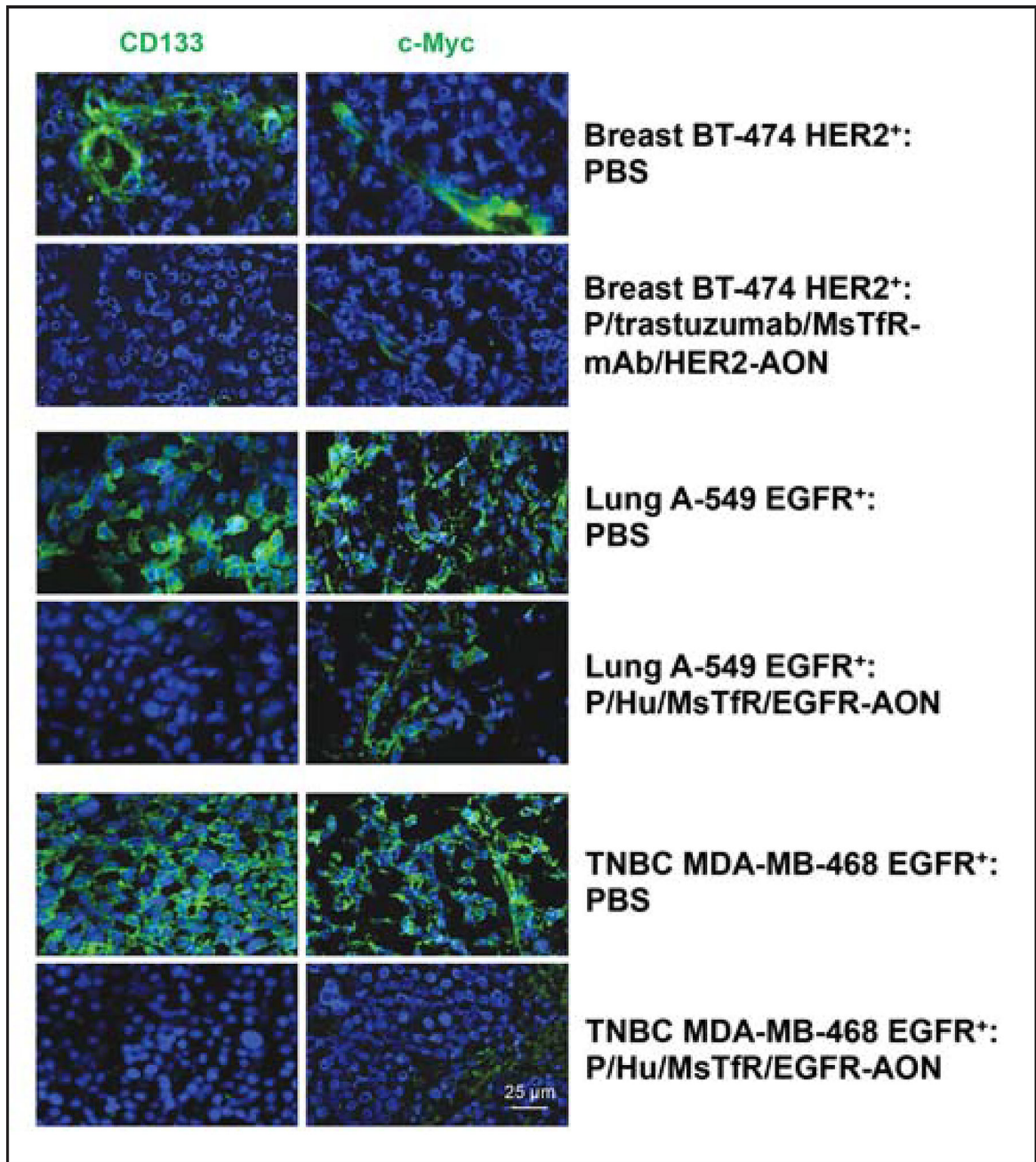**Figure 4.**

Figure 5.

Figure 6.

Figure 7.
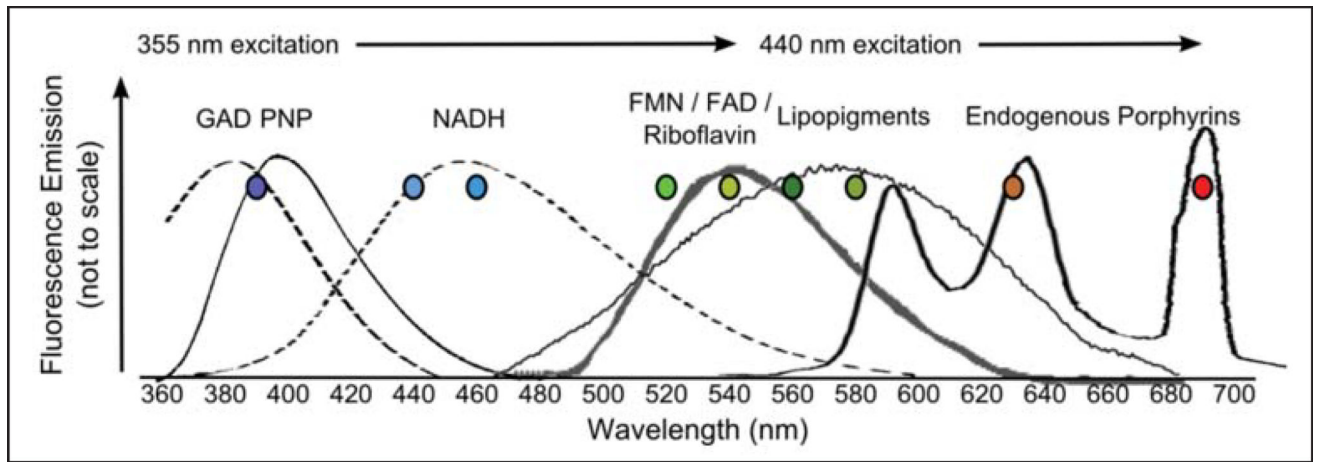
Figure 8.
Natural fluorophores of biological tissue.
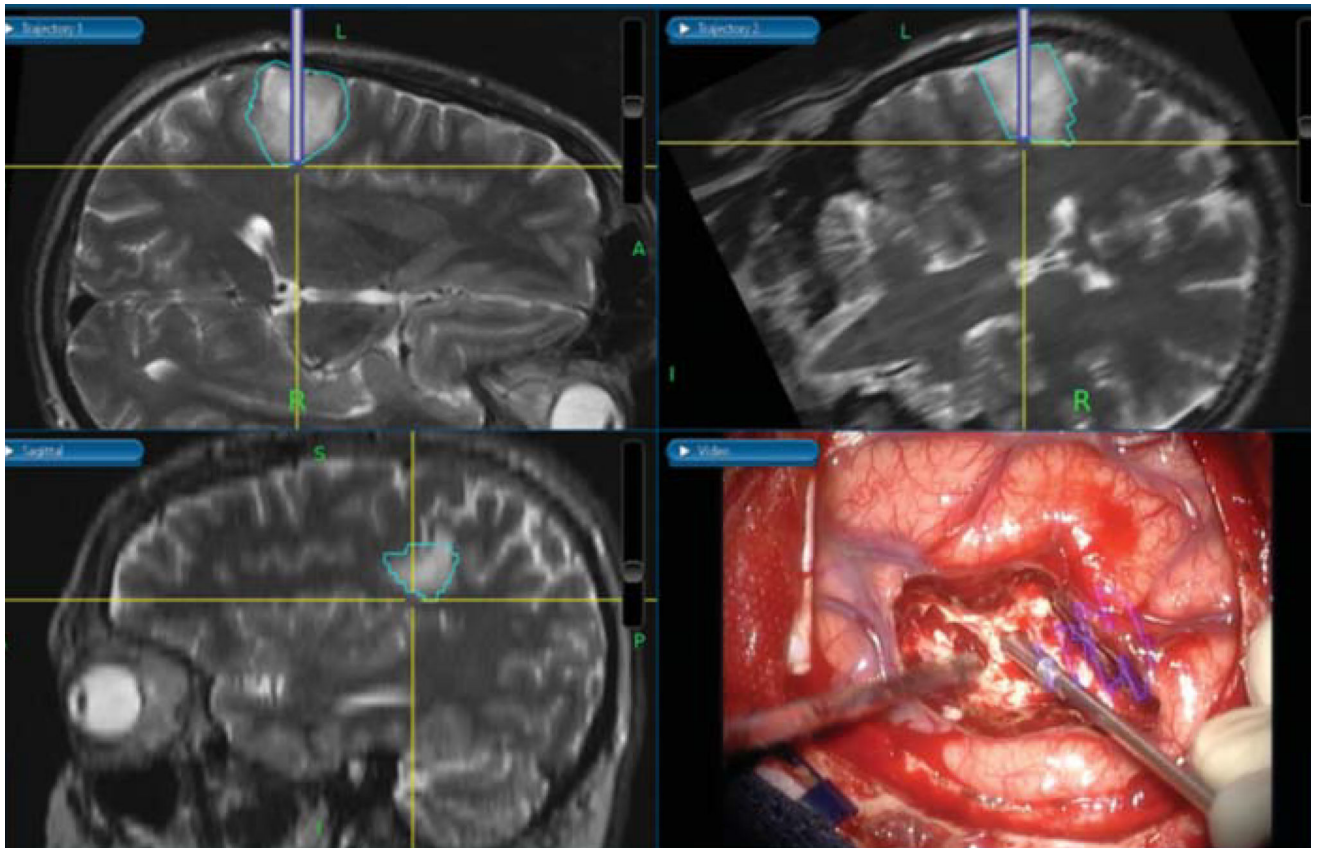
Figure 9.
TRFS measurement registered by neuro-navigation.
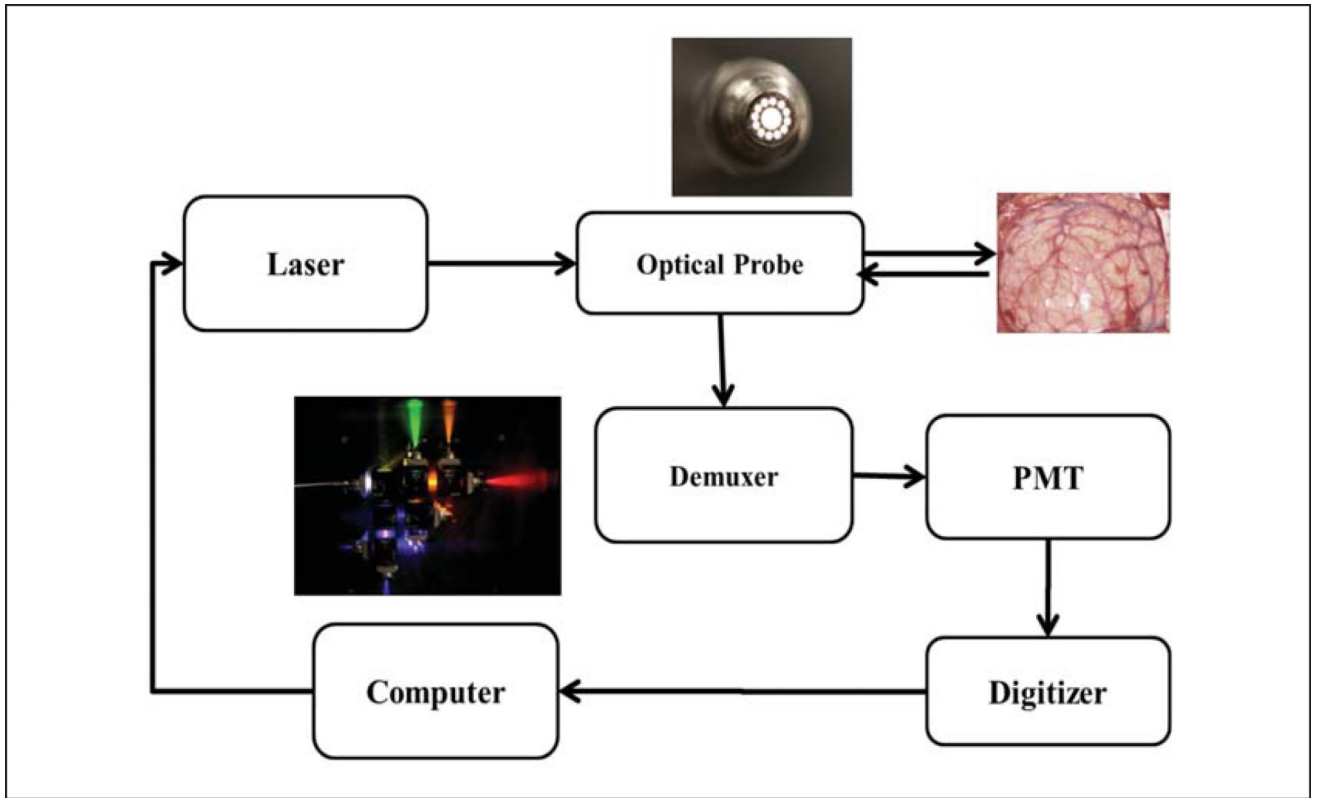
Figure 10.
TRFS system diagram.
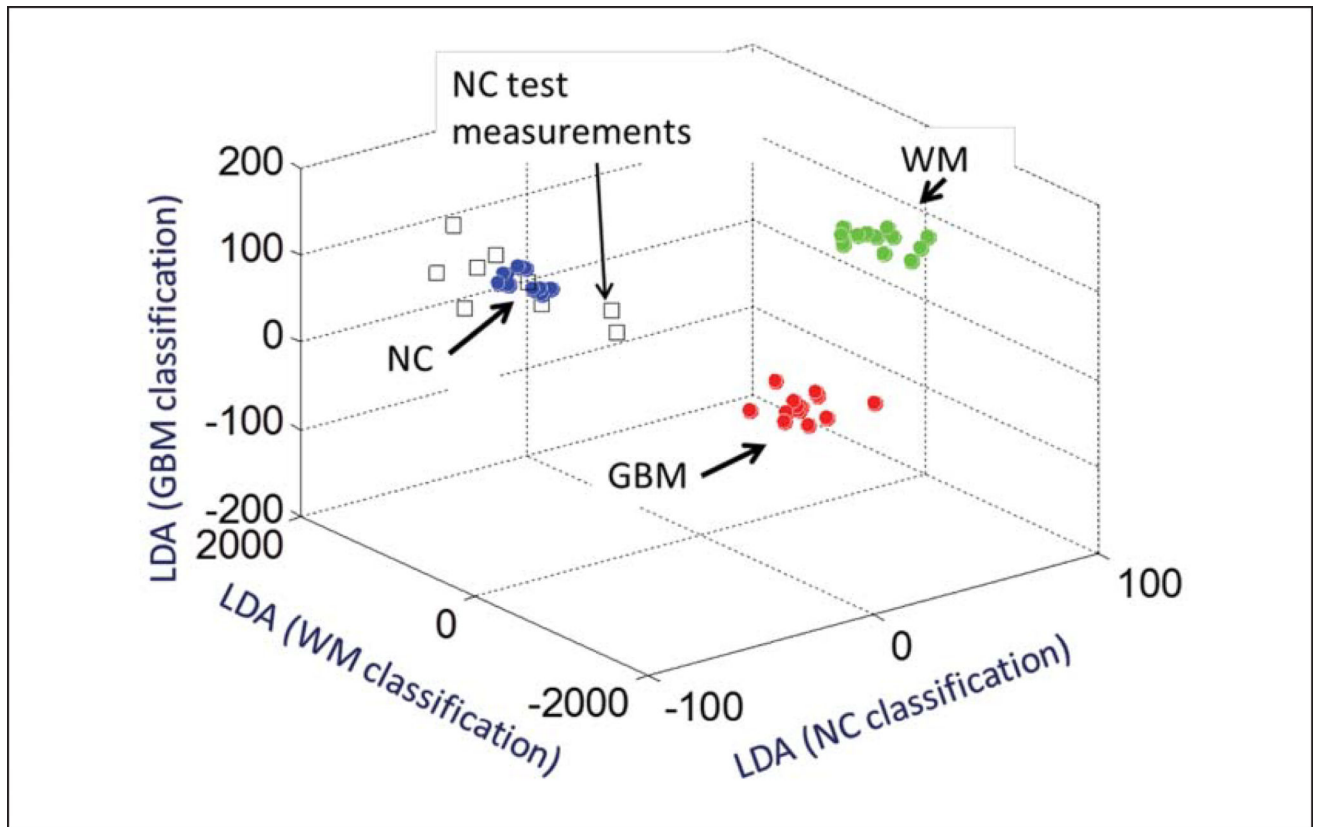
Figure 11.
TRFS Classification output for differentiating, Normal Cortex, White Matter, and GBM tissue types.
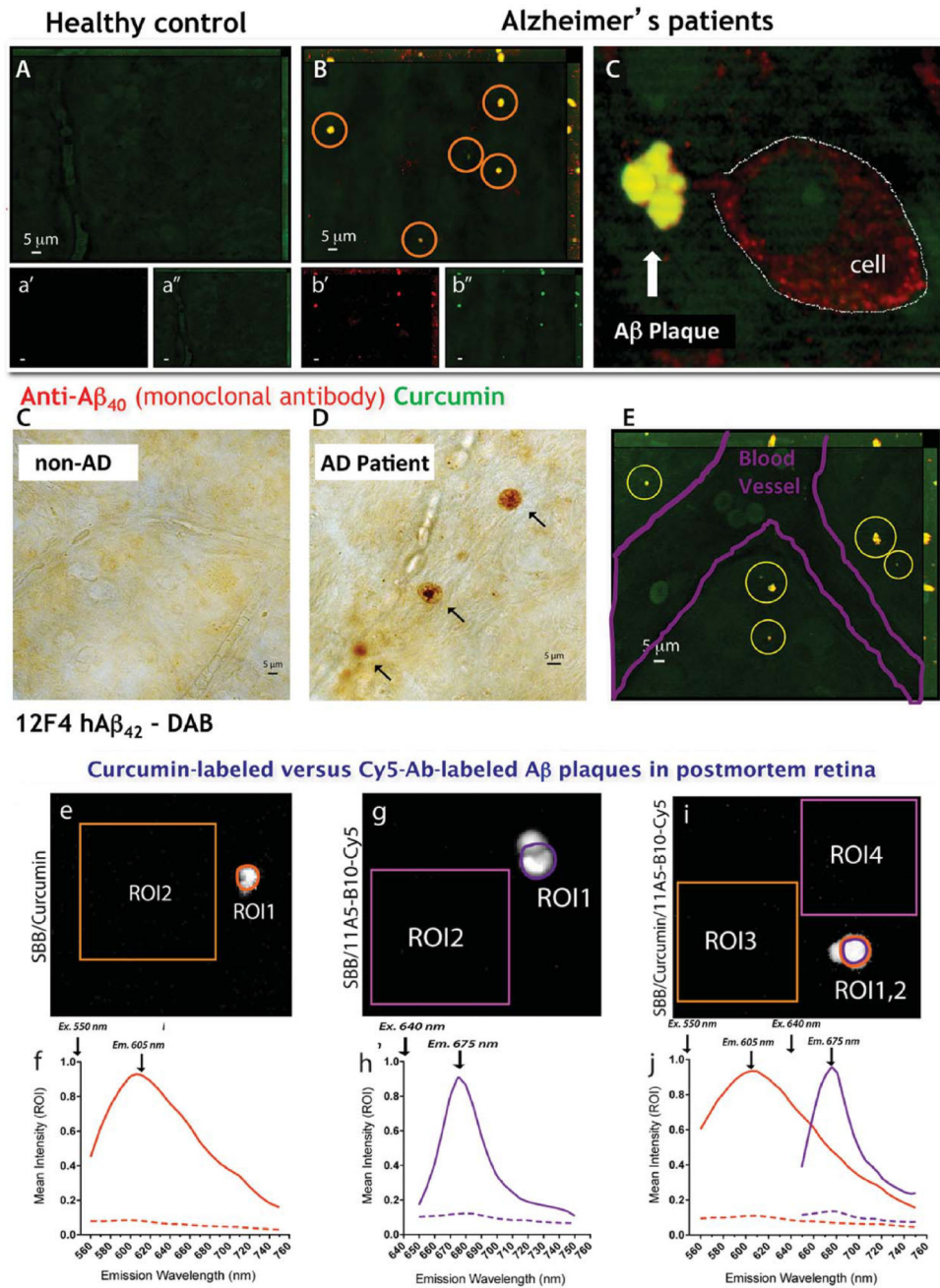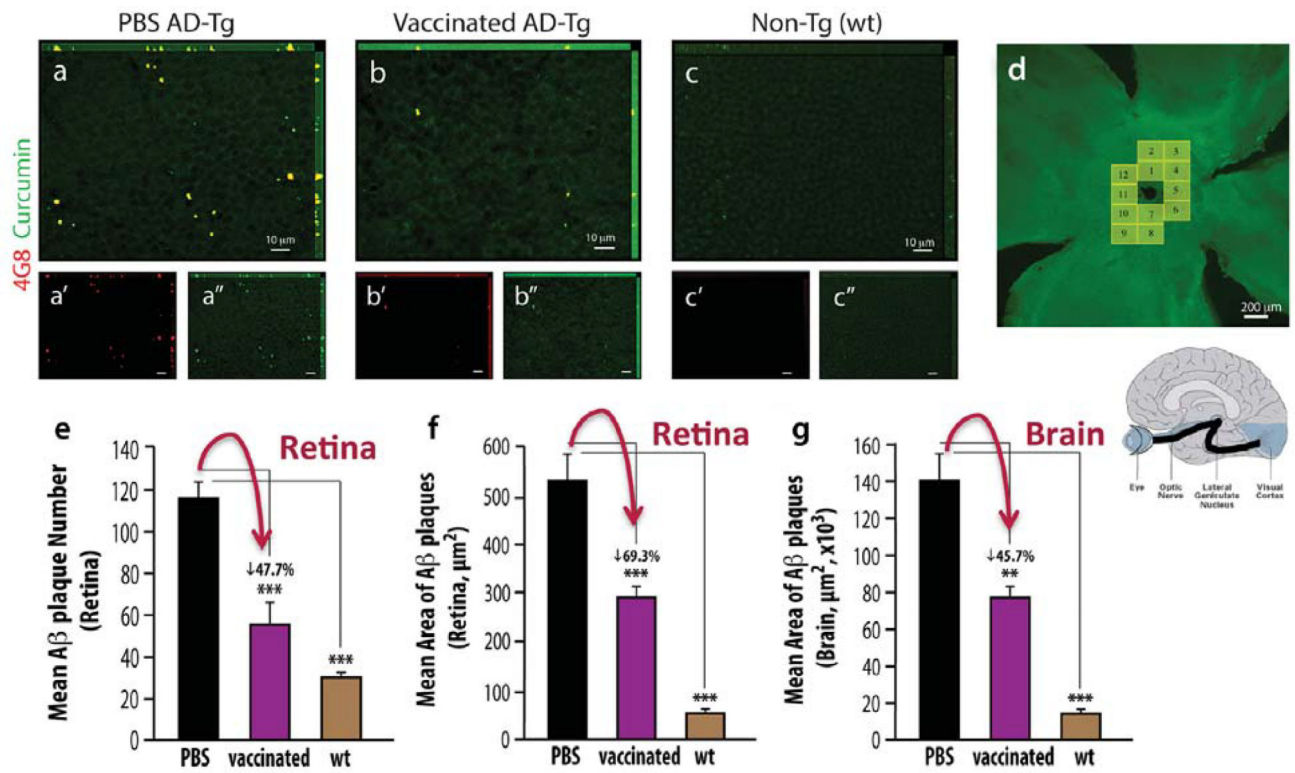
Figure 12.
Koronyo-Hamaoui et al., NeuroImage 2011.

Non-AD (normal) Possible AD (cognitively normal) Possible AD (dementia)

Possible AD (MCI) Probable AD (dementia) AD Definite (severe late-stage)
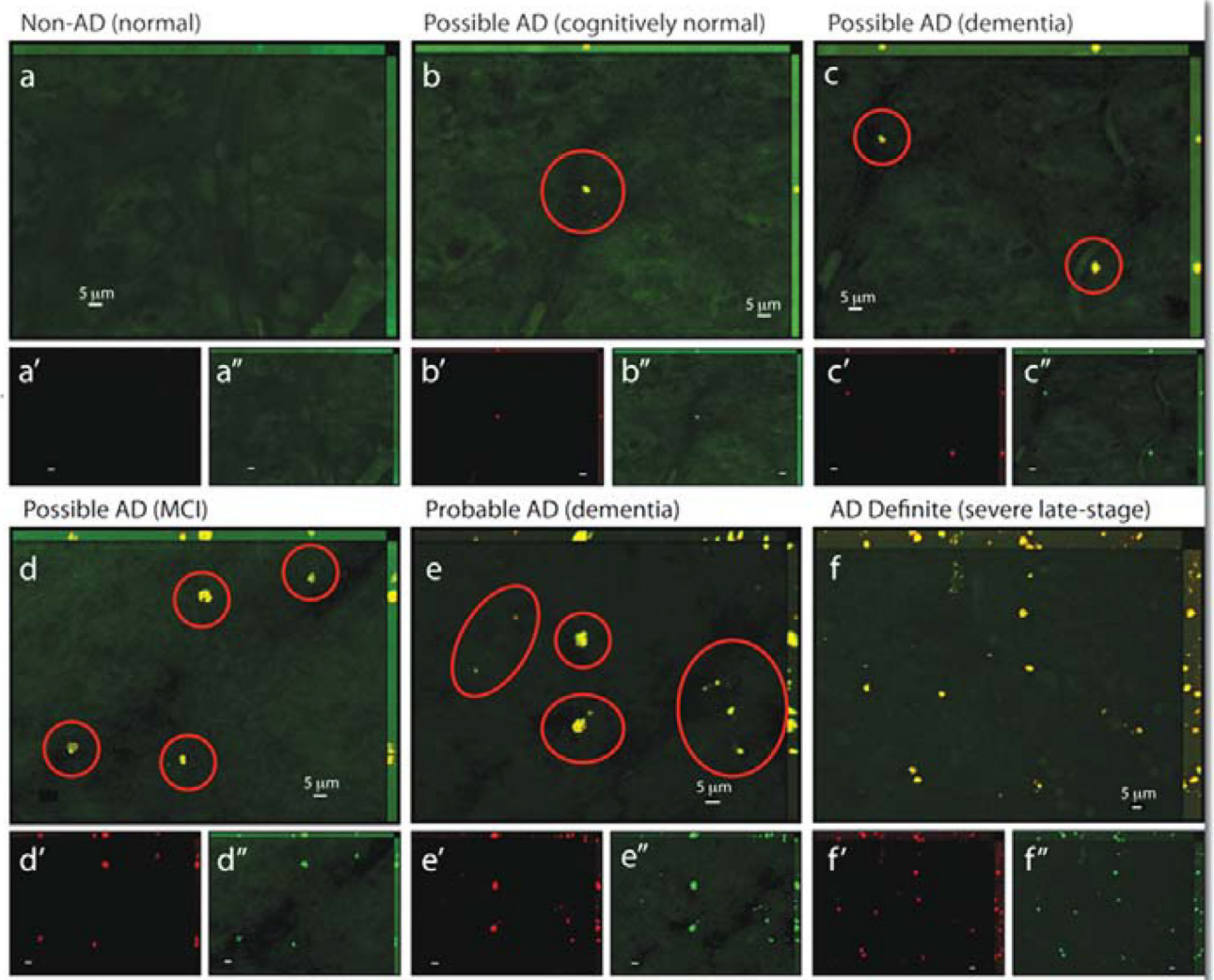
Anti-Aβ$_{42}$ mAb Curcumin

Koronyo-Hamaoui et al., NeuroImage 2011

Figure 13.
Hallmark plaques detected early in the retina of AD patients.

Figure 14.
Quantitative Assay: amyloid-beta plaque reduction in the retina to the same extent as in the brain in response to immunomodulation therapy.
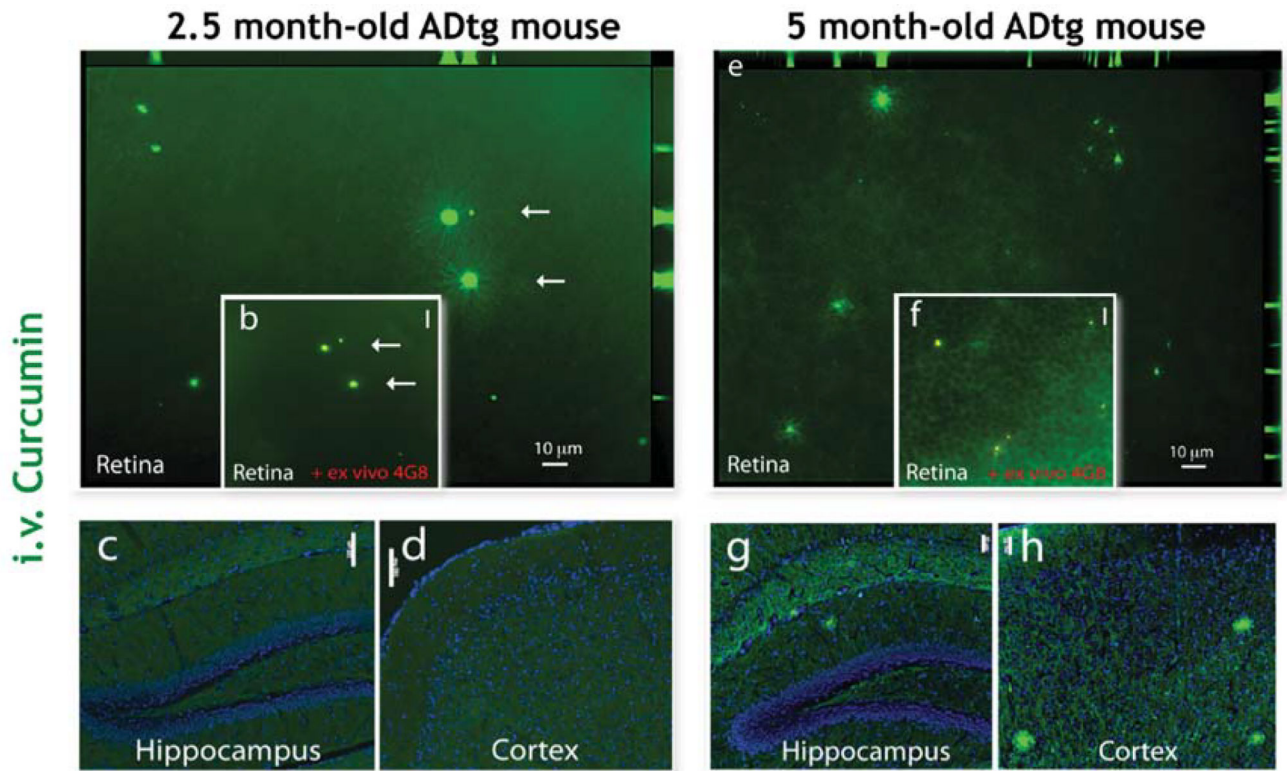
Koronyo-Hamaoui et al., NeuroImage 2011

Figure 15.
Accumulation of amyloid-bete deposits in the retina with disease progression in ADtg mice;
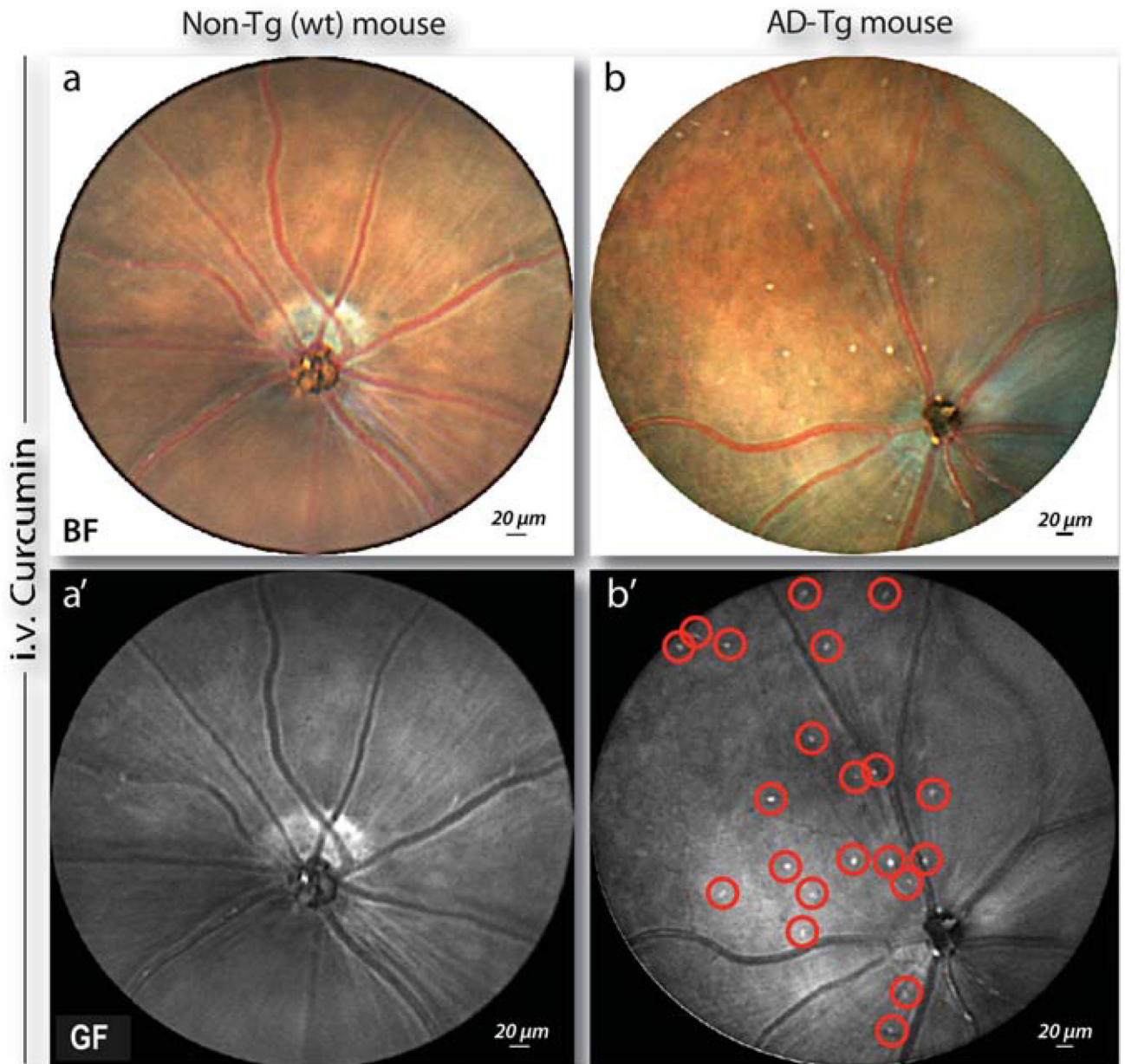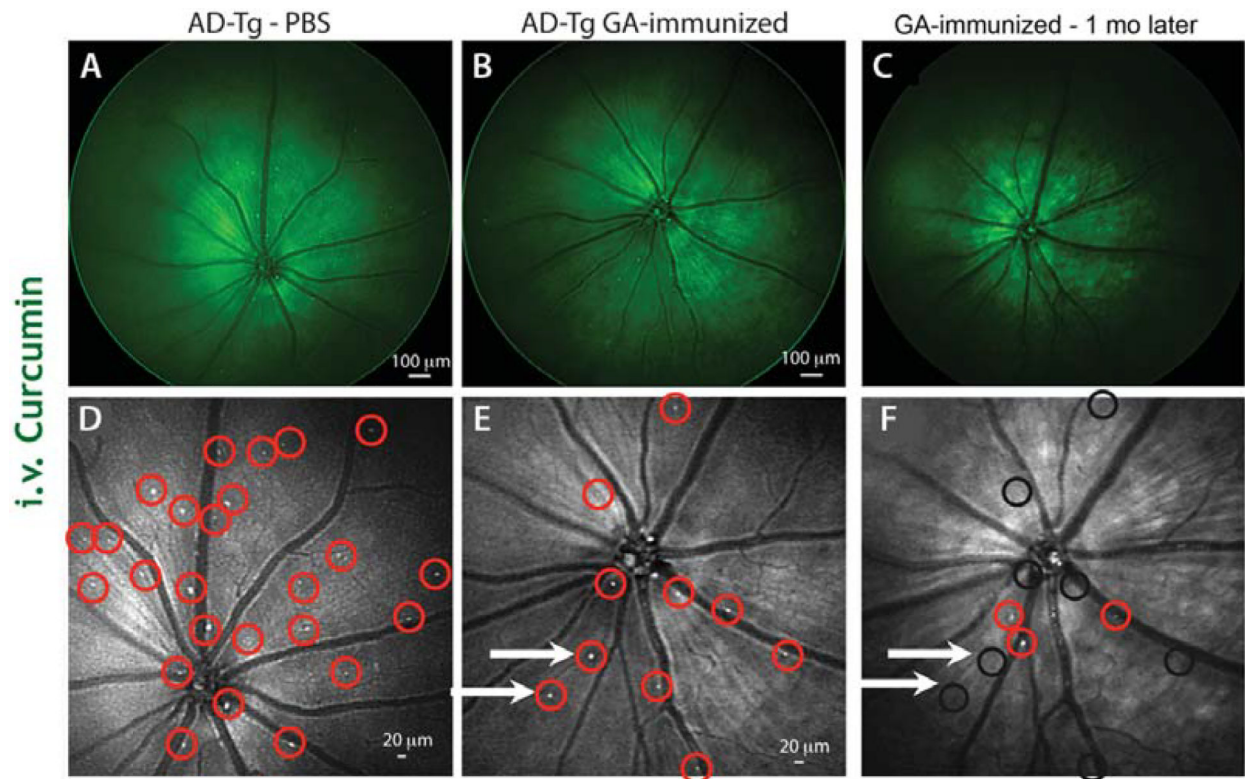Earlier detection of plaques in the retina than in the brain.

Figure 16.

Longitudinal study of curcumin-labeled Aβ plaques in the mouse retina following glatiramer acetate (GA)-immunotherapy. Intravenous (i.v.) injection of curcumin to ADtg mouse allows visualizing *in vivo* retinal Aβ plaques. Images A – C are in green fluorescence (GF) channels, D – F are the same images magnified and in gray scale . White spots are Aβ plaques. Image D shows AD-Tg mouse treated with PBS where Aβ plaques are indicated by red circles. After a month of GA treatment a reduction in Aβ plaques is observed (Image E). After another month of GA, we monitored dynamic changes in distinct retinal Aβ plaques (Image F). Noticeable decrease in Aβ plaques as indicated by black circles and as marked by white arrows and appearance of new Aβ plaques as indicated by red circles.

Koronyo et al., Neurodegenerative Dis. 2012

Figure 17.

Table 1

Summary of nanoconjugates: their abbreviations and physicochemical characterization.

Imaging and treatment agents	Hydrodynamic diameter (nm)[a]	Zeta potential (mV)[b]
poly($\updownarrow$-L-malic acid) (PMLA)	6.6 (±0.1)	−22.9 (±1.7)
P/MEA(4%)/Gd-DOTA(10–12%)[c] (Preconjugate-1)	8.8 (±0.7)	−16.8 (±1.8)
P/cetuximab(0.12%)/MsTfR-mAb(0.12%)/Alexa-680(1%)/Gd-DOTA(10–12%) (P/Gd-DOTA/cetuximab/MsTfR-mAb/Alexa-680)	16.0 (±1.5)	−8.7 (±1.2)
P/trastuzumab(0.12%)/MsTfR-mAb(0.12%)/Alexa-680 (1%)/Gd-DOTA(10–12%) (P/Gd-DOTA/trastuzumab/MsTfR-mAb/Alexa-680)	16.3 (±1.6)	−6.9 (±1.1)
P/mPEG(5%)/LOEt(40%)/MEA(4–6%) (Preconjugate-2)	8.1 (± 0.5)	−8.45 (±1.2)
P/mPEG(5%)/LOEt(40%)/HuTfR-mAb(0.2%)/ MsTfRmAb(0.2%)/EGFR-AON(2–4%) (P/Hu/MsTfR-mAb/EGFR-AON)	15.7 (± 2.0)	−2.61 (±0.8)
P/mPEG(5%)/LOEt(40%)/trastuzumab(0.2%)/MsTfR (0.2%)/HER2 AON(3–4%) (P/trastuzumab/MsTfR-mAb/HER2-AON)	15.7 (± 2.0)	−4.09 (±.8)

[a]Hydrodynamic diameter by number distribution at 25°C measured in PBS at a concentration of 2 mg/ml, calculated from DLS data by Malvern Zetasizer software (Malvern Instruments, Malvern, UK), which assumes spherical shapes of particles.

[b]zeta potential at 25°C in aqueous solution of 10 mM NaCl at 150 mV.

[c]composition of nanoconjugates; percentage refers to total number (100%) of pendant carboxyl groups in unsubstituted PMLA.